JETIR.ORG ISSN: 2349-5162 | ESTD Year : 2014 | Monthly Issue
JOURNAL OF EMERGING TECHNOLOGIES AND INNOVATIVE RESEARCH (JETIR)
An International Scholarly Open Access, Peer-reviewed, Refereed Journal

NGS, MOLECULAR DOCKING AND NETWORK PHARMACOLOGY REVEAL POTENT INHIBITOR FOR THE TREATMENT OF LUNG CANCER

Shipra Chaudhary[1], Uma Kumari[2]

[1]Project Trainee, Bioinformatics Project and Research Institute, Noida-201301,India

[2]Senior Bioinformatics Scientist, Bioinformatics Project and Research Institute, Noida -201301, India

Corresponding Author:Uma Kumari (uma27910@gmail.com)

Abstract: Lung cancer, particularly non-small cell lung cancer (NSCLC), remains a leading cause of cancer mortality worldwide. Among the molecular drivers of NSCLC, mutations in the KRAS gene, specifically the G12C mutation, have emerged as a critical target for therapeutic intervention. However, developing inhibitors for this "undruggable" mutation has been historically challenging. In this study, an integrated computational approach combining Next-Generation Sequencing (NGS), molecular docking, and network pharmacology was used to identify novel inhibitors targeting the KRAS G12C protein (PDB ID: 6USZ). NGS data was utilized to characterize mutations in the KRAS protein associated with NSCLC, highlighting the G12C mutation as a potential therapeutic target. Using CB-Dock for molecular docking simulations, several small molecules were screened for their ability to bind to the active site of 6USZ. The docking results revealed that compounds Remdesivirand Adagrasib exhibited the highest binding affinities and favorable interactions with key residues in the G12C mutant protein. Structural analyses were performed using PyMOL and MolProbity to visualize and validate the protein-ligand interactions.

Keywords: KRAS G12C Mutation; Lung Cancer; Molecular Docking; PDB 6USZ; Computational Drug Discovery

Introduction

Lung cancer accounts for around 18% of all cancer-related deaths globally, making it one of the most common and deadly malignancies. It is classified into two main types: non-small cell lung cancer (NSCLC) and small cell lung cancer (SCLC), of which roughly 85% of cases are NSCLC. Adenocarcinoma, Squamous Cell Carcinoma, and Large Cell Carcinoma are further subtypes of Non-Small Cell Lung Cancer. Adenocarcinoma is the most common histological subtype among them. Lung cancer patients frequently have a poor prognosis despite improvements in early diagnosis and treatment, primarily because of late-stage discovery and the emergence of resistance to conventional medicines like radiation and chemotherapy. Some individuals have had better results from current targeted therapy, such as ALK kinase inhibitors and epidermal growth factor receptor (EGFR) inhibitors. ALK kinase inhibitors, have provided improved outcomes for some patients. However, acquired resistance to these therapies, as well as the high rate of somatic mutations in lung cancer genomes, complicates treatment strategies [1, 2].

One of the main cause of lung cancer, especially in KRAS-mutant NSCLC, is the KRAS gene, which belongs to the RAS family of GTPases. KRAS mutations, particularly the KRAS G12C mutation, are prevalent in about 30% of NSCLC cases. The mutated KRAS gene leads to uncontrolled cell proliferation, survival, and differentiation by continuously activating the MAPK and PI3K/AKT signaling pathways. As a result, KRAS-driven lung cancers exhibit aggressive progression and resistance to standard treatments. Historically, KRAS mutations have been considered "undruggable" due to the difficulty in targeting the protein's active site with small molecules, which has a high affinity for GTP and lacks a well-defined binding pocket.However, recent breakthroughs in covalent inhibitors have reignited interest in targeting this mutation, offering hope for new therapeutic approaches. One such breakthrough is the development of KRAS G12C inhibitors, which specifically target the mutant KRAS protein in its inactive GDP-bound state, effectively halting the downstream signaling that drives tumor growth. The emergence of KRAS G12C as a key target has led to the development of inhibitors such as MRTX849, which bind covalently to the cysteine at position 12 (Cys12). This approach has paved the way for the rational design of small molecules that lock KRAS G12C in its inactive state, thus inhibiting its oncogenic activity[3, 4].

The protein 6USZ represents the crystal structure of KRAS in complex with MRTX849, a covalent inhibitor specifically designed to target the G12C mutation. This structure has become a crucial model for understanding how inhibitors bind to the KRAS G12C mutant protein and offers valuable insights for developing novel inhibitors. Structural analyses of 6USZ using advanced bioinformatics and molecular modeling tools such as PyMOL and PDBePISA have revealed critical insights into the active site, binding pockets, and druggable regions of the protein. This structural knowledge is indispensable for rational drug design aimed at creating more effective inhibitors for KRAS-mutant lung cancer[4, 5].

The rapid evolution of computational methods has significantly impacted the field of drug discovery, enabling the identification of new therapeutic compounds with unprecedented speed and accuracy. Molecular docking, and virtual screening are essential tools used to predict how small molecules (inhibitors) interact with their target proteins. Molecular Docking simulates the binding of a small molecule (e.g., a drug or ligand) to the active site of a target protein, predicting the orientation, binding affinity, and interactions between the molecule and protein residues.

In this study, CB-Dock, a well-established molecular docking tool, was used to screen potential inhibitors for 6USZ, assessing their binding affinities and identifying key interactions that contribute to the inhibitory activity.While molecular docking and NGS provide valuable insights into protein-ligand interactions and mutational landscapes, network pharmacology offers a broader systems-level understanding of drug-target interactions. Network pharmacology integrates data from various biological networks, such as protein-protein interactions, gene-drug interactions, and metabolic pathways, to assess the systemic effects of potential inhibitors. This holistic approach not only identifies promising drug candidates but also predicts off-target effects and interactions within the broader biological network. This research offers a multi-disciplinary approach to drug discovery for lung cancer, combining state-of-the-art computational tools with experimental data to identify novel therapeutic strategies. The identification of potent inhibitors targeting the 6USZ protein could lead to the development of more effective treatments for patients with KRAS-driven NSCLC, addressing a critical unmet need in cancer therapy. By integrating structural biology, computational chemistry, and systems pharmacology, this study aims to provide a comprehensive framework for understanding the molecular basis of KRAS-driven lung cancer and developing targeted therapies that overcome the challenges associated with traditional treatment approaches [6, 7, 8].

Material and Methods

The KRAS G12C mutant protein (PDB ID: 6USZ) was selected from the Protein Data Bank (PDB) due to its critical role in the progression of non-small cell lung cancer (NSCLC). The 6USZ protein is a structure of KRAS in complex with a covalent inhibitor (MRTX849), which binds selectively to the G12C mutant form of KRAS, making it a prime target for the development of small-molecule inhibitors [8, 9].

To ensure the structural integrity and to visualize the 3D structure of the protein, PyMOL was used. PyMOL provides high-quality 3D visualization of the protein, enabling us to examine key features such as the binding pocket, active sites, and overall folding of the protein. Structural validation of 6USZ was performed using MolProbity to check for steric clashes, rotamer outliers, and the geometry of the protein [10, 11, 12].

Multiple sequence alignment of 6USZ was performed using Clustal Omega, a widely used tool for comparing sequences across homologous proteins. This alignment helped identify conserved regions that are functionally important for KRAS and its role in cellular signaling pathways. By comparing 6USZ with its homologous proteins from different species, we gained insights into evolutionary conserved functional domains. Clustal Omega is a widely used tool for performing multiple sequence alignments (MSA) of DNA, RNA, or protein sequences. It is the latest iteration of the Clustal series, known for its efficiency and accuracy in aligning multiple biological sequences. Multiple sequence alignment is crucial in bioinformatics as it allows researchers to compare homologous sequences, identify conserved regions, and infer evolutionary relationships between species or within gene families [13, 14].To complement the sequence alignment, a BLAST (Basic Local Alignment Search Tool) analysis was conducted to compare the 6USZ sequence against other KRas protein sequences available in the PDB database. BLAST was used to ensure the similarity between the selected sequence and other KRas variants, providing insights into evolutionary relationships and structural conservation. The BLAST results indicated a high level of sequence identity with other KRas homologous proteins (e.g., PDB IDs: 4LRW_A, 6OIM_A, and6T5B_A), confirming that the 6USZ protein is highly representative of KRas sequences involved in NSCLC. This validation ensures that the structural features of 6USZ are conserved across homologous proteins, making it an ideal candidate for drug docking and inhibitor screening [15].

Additionally, PSIPRED, a secondary structure prediction tool, was employed to predict the α-helices, β-sheets, and coil regions of the 6USZ protein. This prediction confirmed the structural elements of the protein, which were then mapped onto the 3D model to understand its functional regions and assess its potential druggable sites. PSIPRED is a widely used bioinformatics tool designed to predict the secondary structure of proteins based on their amino acid sequence. It provides accurate predictions of whether regions of a protein are likely to form α-helices**,** β-sheets, or coil regions[16, 17].Next-Generation Sequencing (NGS) data from lung cancer patients was analyzed to identify mutations in the KRAS gene, particularly those affecting the G12C mutation. NGS data from public databases such as COSMIC (Catalogue of Somatic Mutations in Cancer) was utilized to cross-reference the identified mutations and assess their frequency and clinical relevance in NSCLC. COSMIC provided detailed mutation profiles for KRAS, enabling the identification of common mutational hotspots [18, 19].

Molecular docking simulations were performed using CB-Dock, an automated docking tool that identifies the optimal binding sites of small molecules on target proteins. The docking study was conducted to evaluate the binding affinities of various potential inhibitors against the 6USZ protein. CB-Dock was selected for its ability to predict the top-ranking binding pockets and generate docking scores based on the interaction energy between the ligand and protein [20].

Result and Discussion

1. Structural Analysis of protein

Table 1: MolProbity Result

Category	Metric	Value	Goal
Protein Geometry	Poor rotamers	3 (2.00%)	<0.3%
	Favoredrotamers	136 (90.67%)	>98%
	Ramachandran outliers	1 (0.60%)	<0.05%
	Ramachandranfavored	161 (96.41%)	>98%
	Rama distribution Z-score	-0.51 ± 0.61	abs(Z score) < 2
	Cβ deviations>0.25Å	6 (3.77%)	0
	Bad bonds	4 / 1451 (0.28%)	0
	Bad angles	10 / 1966 (0.51%)	<0.1%
Peptide Omegas	CisProlines	0 / 4	0

Additional Validations	Chiral volume outliers	0 / 215	Expected: ≤1 per chain or <5%

Protein Geometry: The 6USZ structure shows a slightly higher number of poor rotamers (2.00%) compared to the goal (<0.3%). Ramachandran plot analysis indicates a favorable geometry with 96.41% of residues in favored regions, but with one outlier (0.60% vs. a goal of <0.05%). The Cβ deviations (3.77%) and bad bonds (0.28%) show minor deviations from the ideal structure, but overall, the protein maintains a good structural integrity.

Peptide Omegas: No cisprolines were detected, ensuring proper peptide bond geometry.

Additional Validations: No chiral volume outliers were found, indicating proper stereochemistry for all chiral centers in the structure.

Structure 1				×	Structure 2						interface	ΔiG	ΔiG	N_{HB}	N_{SB}	N_{DS}	CSS
Range	$^{i}N_{at}$	$^{i}N_{res}$	Surface Å^2		Range	Symmetry op-n	Sym.ID	$^{i}N_{at}$	$^{i}N_{res}$	Surface Å^2	area, Å^2	kcal/mol	P-value				
[QH4]A:203	40	1	832	cf	A	x,y,z	1_555	83	27	8296	554.4	-1.9	0.448	3	0	0	0.011
A	52	15	8296	x	A	-x+1,y-1/2,-z-1/2	3_644	54	14	8296	437.5	-0.7	0.621	6	2	0	0.000
[GDP]A:201	27	1	565	f	A	x,y,z	1_555	50	18	8296	353.3	-7.7	0.486	13	0	0	0.046
A	17	5	8296	x	A	x-1,y,z	1_455	20	10	8296	150.6	0.8	0.735	3	0	0	0.000
A	15	4	8296	x	A	x-1/2,-y-1/2,-z	4_445	19	5	8296	128.2	-1.8	0.301	1	0	0	0.000
A	12	4	8296	x	A	x-1/2,-y+1/2,-z	4_455	12	4	8296	104.0	0.2	0.646	2	0	0	0.000
A	13	4	8296	◊	[QH4]A:203	-x+1,y-1/2,-z-1/2	3_644	5	1	832	73.4	-0.1	0.505	0	0	0	0.000
[MG]A:202	1	1	98	f	A	x,y,z	1_555	14	8	8296	45.5	-6.6	0.000	0	0	0	0.023
A	10	2	8296	◊	[GDP]A:201	x-1,y,z	1_455	6	1	565	43.2	0.3	0.652	0	0	0	0.000
[MG]A:202	1	1	98	f	[GDP]A:201	x,y,z	1_555	4	1	565	29.2	-4.4	0.000	0	0	0	0.015
[QH4]A:203	2	1	832	f	[GDP]A:201	x,y,z	1_555	3	1	565	24.5	-1.0	0.494	0	0	0	0.004
A	1	1	8296	x	A	-x,y-1/2,-z-1/2	3_544	1	1	8296	7.6	0.2	0.796	0	0	0	0.000
[QH4]A:203	1	1	832	f	[MG]A:202	x,y,z	1_555	1	1	98	4.2	-0.3	0.000	0	0	0	0.001

Figure 1: PDBePISA result

The PISA analysis reveals that several interfaces within the crystal structure exhibit a variety of interaction strengths, from moderate to weak. The strongest interaction is seen at the symmetry-related interface involving chain A:203, with a ΔG of -7.7 kcal/mol. These interactions suggest a stable complex, particularly at specific interfaces, which may contribute to the overall biological function of the protein complex under study.

This analysis contributes to understanding the binding characteristics and interface stability within the structure of 6USZ, which may have implications for the development of inhibitors or therapeutic molecules targeting this protein complex.

2. Sequence Analysis

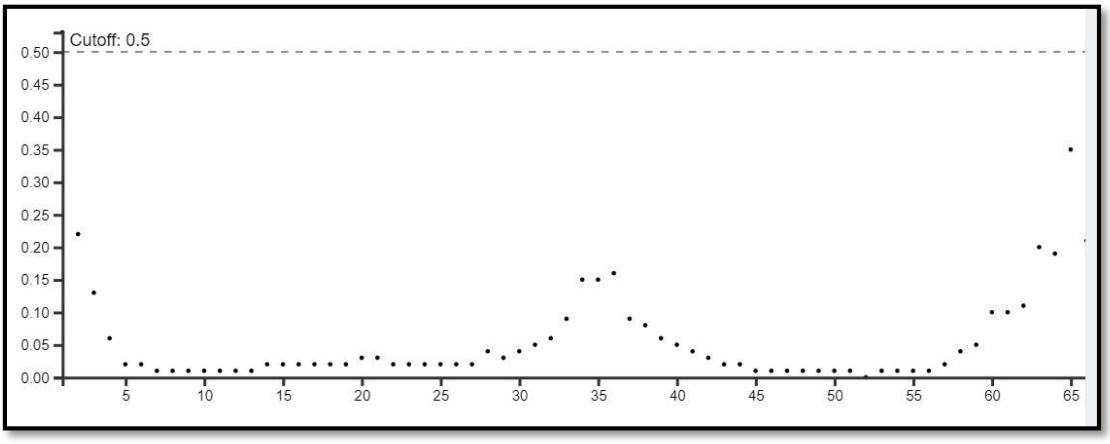

Figure 2: DISOPRED3 Plot Analysis obtained through PSIPRED

- Most residues fall well below the 0.5 cutoff, indicating that the majority of the protein structure is predicted to be ordered.
- Around residues 35 to 40, there is a moderate peak in disorder probability (close to 0.3–0.4), indicating that this region may exhibit some flexibility or partial disorder.
- Residues after position 60 show a slight increase in disorder probability, though they remain below the 0.5 threshold.

In summary, no significant disorder is predicted in the 6USZ protein structure based on this DISOPRED3 plot, suggesting the protein is largely ordered, with minor flexibility in some regions.

Description	Scientific Name	Max Score	Total Score	Query Cover	E value	Per. Ident	Acc. Len	Accession
Chain A, GTPase KRas [Homo sapiens]	Homo sapiens	351	351	100%	7e-122	100.00%	170	4LRW_A
Chain A, GTPase KRas [Homo sapiens]	Homo sapiens	351	351	100%	1e-121	100.00%	183	6OIM_A
Chain A, GTPase KRas [Homo sapiens]	Homo sapiens	350	350	100%	2e-121	99.41%	170	6T5B_A

Figure 3: Sequence Similarity analysis of GTPase KRas homosapiens proteomic sample

The BLAST results demonstrate a strong alignment between the query sequence and the KRas protein variants. Both **4LRW_A** and **6OIM_A** are exact matches, while **6T5B_A** shows minimal variation with a slightly lower percentage identity (99.41%).All three entries have very low **E-values** of **7e-122** for 4LRW_A and 6OIM_A, and **2e-121** for 6T5B_A. These values indicate highly significant matches between the query sequence and the subject sequences, with essentially no chance of the matches being random.All sequences have **100% query coverage**, meaning the entire length of the query sequence aligns with the subject sequences without any gaps or missing sections.

Figure 4: Multiple Sequence Alignment Result obtained through Clustal Omega

The provided sequences represent variants of the GTPaseKRas protein from different PDB entries (6USZ, 4LRW, 6OIM, and 6T5B). The alignment reveals the evolutionary relationship between these sequences. The phylogenetic tree (phylogram) clearly shows that pdb|6T5B|A diverges slightly from the other three sequences, which have identical alignments. This divergence is represented by a longer branch length of 0.00588 in the phylogram, indicating a slight evolutionary distance between pdb|6T5B|A and the rest.

The slight evolutionary divergence observed in the phylogram and the highly conserved sequence among the different PDB entries indicates that these KRas protein structures are functionally similar, with some minor variations that might not greatly affect the protein's overall function. These findings suggest that the proteins retain their functional roles in GTP binding and hydrolysis, but minor structural variations may have implications for protein-protein interactions, particularly in the context of targeted drug design or protein engineering.

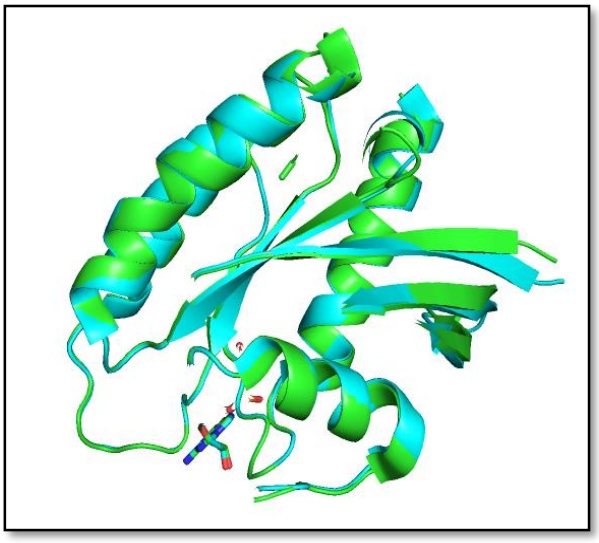

Figure 5:Protein-Protein Interaction between two proteomic lung cancer sample showing Rmsd 0.4 Angstrom indicate very close structural similarity are nearly identical with only minor deviations (6USZ,6OIM)

This low RMSD value suggests that the overall backbone structure and folding of the two KRas protein samples are highly conserved. Minor structural differences might be present in side chains or loop regions, but the core secondary structure (helices and beta sheets) is almost identical.The superimposed protein structures in cyan and green demonstrate close alignment between the two models, which is particularly relevant for understanding the consistency of KRas's role in cancer across different samples or experimental conditions.

The structural comparison between 6USZand 6OIMreveals that both KRas variants share a highly similar 3D conformation, with an RMSD of 0.4 Å, indicating strong conservation of the functional regions. This level of similarity suggests that the KRas proteins from different sources (or under different experimental conditions) are structurally robust, which is crucial for developing broad-acting inhibitors targeting KRas-driven lung cancers.

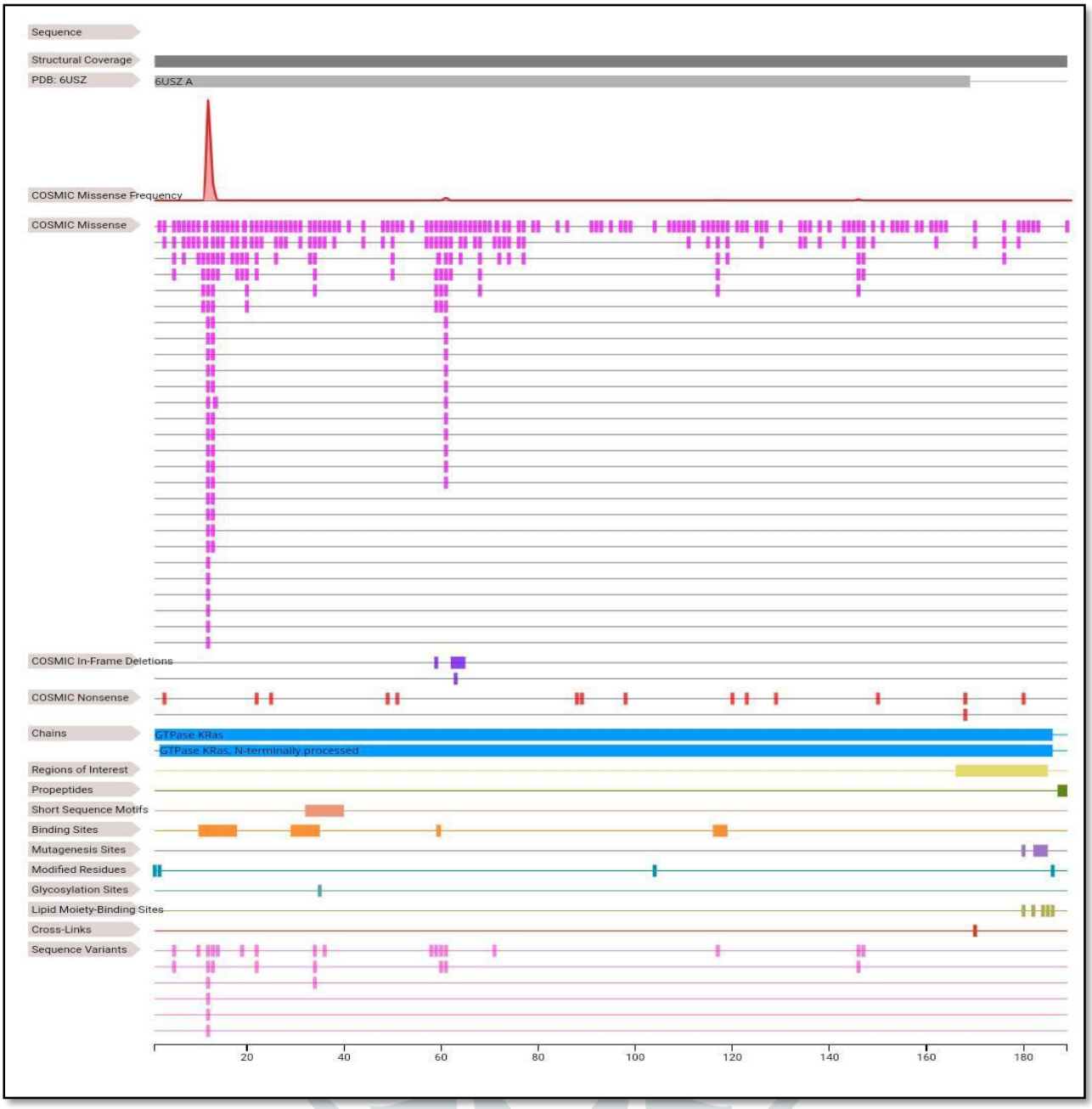

Figure 6: COSMIC Result

The chart shows a high density of missense mutations across the KRas protein sequence. The peak in the red line under the "COSMIC Missense Frequency" section suggests that certain positions within the sequence are hotspots for somatic mutations in cancer. The purple bars represent the positions of missense mutations. These mutations alter the amino acid sequence and can disrupt the protein's normal function, potentially leading to oncogenic activation or loss of regulation.

- **Position 12** in the KRas sequence shows the highest mutation frequency with a count of **39,180**. The high frequency of missense mutations at this location underscores its critical role in the KRasGTPase function and its impact on the oncogenic potential of KRas mutations.
- **Position 11**: Lower frequency with a count of **8**.
- **Position 13**: Significant mutation hotspot with **6,892** cases.
- **Position 14**: A lesser but still notable mutation frequency with **52** cases.

These positions are part of the **P-loop region** (phosphate-binding loop) of the GTPase domain, critical for binding and hydrolysis of GTP. Mutations in this region typically result in constitutive activation of KRas, leading to uncontrolled cell proliferation.

3. Molecular Docking

Two drugs has been selected from the virtual screening showing maximum score of binding affinity. First one is Remdesivir (pubchem id: 121304016) and second one is Adagrasib(pubchem id: 138611145).

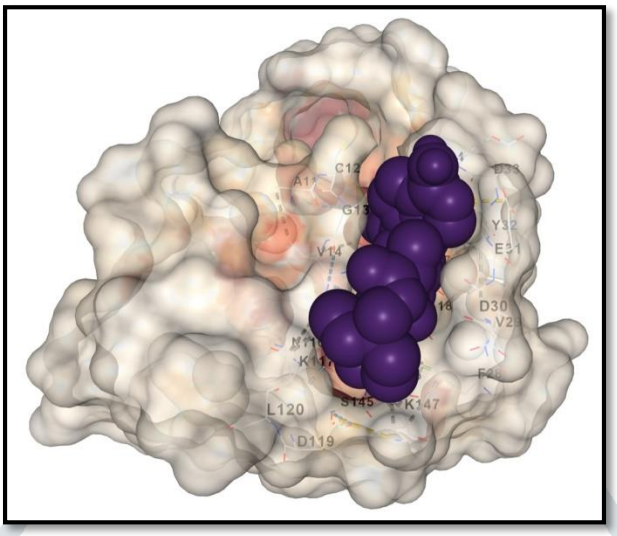

Figure 7: Docked image of protein 6USZ with Remdesivir

Table 2: Docking Result

CurPocket ID	Vina Score	Cavity Volume (Å³)	Center (x, y, z)	Docking Size (x, y, z)
C5	-8.2	34	(31, 5, -13)	(25, 25, 25)
C1	-7.6	1146	(24, -1, -16)	(25, 25, 25)
C2	-6.2	372	(9, 8, -11)	(25, 25, 25)
C3	-6.1	76	(13, -7, -22)	(25, 25, 25)
C4	-5.5	72	(4, 1, -17)	(25, 25, 25)

CurPocket C5 had the best binding affinity with a Vina score of -8.2**,** indicating a stronger potential interaction between the compound and the protein. It is located in a smaller cavity volume (34 Å³) compared to other pockets but has a strong binding energy. The key residues involved in pocket C5 of Chain A are: ALA11, CYS12, GLY13, VAL14, GLY15, LYS16, SER17, ALA18, LEU19, PHE28, VAL29, ASP30, GLU31, TYR32, ASP33, PRO34, ASN85, ASN116, LYS117, SER118, ASP119, LEU120, THR144, SER145, ALA146, LYS147

CurPocket C1 had a slightly lower binding affinity than C5, with a Vina score of -7.6**,** but it is located in the largest cavity volume **(**1146 Å³**),** suggesting that it may allow for more flexibility in ligand accommodation.

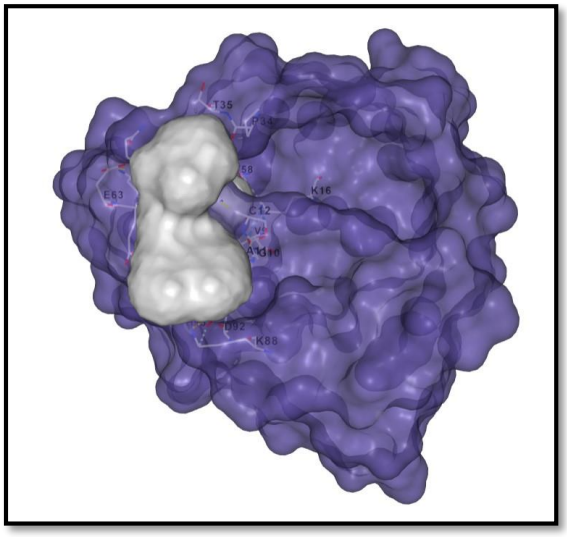

Figure 8: Docked image of protein 6USZ withAdagrasib

Table 3: Docking Result

CurPocket ID	Vina Score	Cavity Volume (Å³)	Center (x, y, z)	Docking Size (x, y, z)
C1	-8.0	1146	(24, -1, -16)	(26, 26, 26)
C3	-7.8	76	(13, -7, -22)	(26, 26, 26)
C5	-7.7	34	(31, 5, -13)	(26, 26, 26)
C2	-6.3	372	(9, 8, -11)	(26, 26, 26)
C4	-6.3	72	(4, 1, -17)	(26, 26, 26)

The key interacting residues within pocket C1 of Chain A include:VAL9, GLY10, ALA11, CYS12, GLY13, VAL14, GLY15, LYS16, SER17, ALA18, PHE28, VAL29, ASP30, GLU31, TYR32, PRO34, THR35, THR58, ALA59, GLY60, GLN61, GLU62, GLU63, TYR64, ARG68, MET72, ASN86, LYS88, SER89, ASP92, HIS95, TYR96, GLN99, ARG102, ASN116, LYS117, ASP119, LEU120, SER145, ALA146, LYS147.

Conclusion

This study offers a comprehensive framework for targeting the KRAS G12C mutation in NSCLC using modern computational methods, highlighting the potential of these identified inhibitors as effective therapeutic candidates for lung cancer treatment. The integration of NGS**,** molecular docking, and network pharmacology opens new avenues for personalized medicine and the development of targeted therapies against previously "undruggable" mutations like KRAS G12C. Further experimental validation of these compounds could lead to breakthroughs in KRAS-driven cancer therapies.

References

1. Fell, J. B., Fischer, J. P., Baer, B. R., Blake, J. F., Bouhana, K., Briere, D. M., Brown, K. D., Burgess, L. E., Burns, A. C., Burkard, M. R., Chiang, H., Chicarelli, M. J., Cook, A. W., Gaudino, J. J., Hallin, J., Hanson, L., Hartley, D. P., Hicken, E. J., Hingorani, G. P., Hinklin, R. J., Marx, M. A. (2020). Identification of the Clinical Development Candidate **MRTX849**, a Covalent KRAS^{G12C} Inhibitor for the Treatment of Cancer. Journal of medicinal chemistry, 63(13), 6679–6693. https://doi.org/10.1021/acs.jmedchem.9b02052
2. Liu, J., Kang, R., & Tang, D. (2022). The KRAS-G12C inhibitor: activity and resistance. Cancer gene therapy, 29(7), 875–878. https://doi.org/10.1038/s41417-021-00383-9

3. Awad, M. M., Liu, S., Rybkin, I. I., Arbour, K. C., Dilly, J., Zhu, V. W., Johnson, M. L., Heist, R. S., Patil, T., Riely, G. J., Jacobson, J. O., Yang, X., Persky, N. S., Root, D. E., Lowder, K. E., Feng, H., Zhang, S. S., Haigis, K. M., Hung, Y. P., Sholl, L. M., Aguirre, A. J. (2021). Acquired Resistance to $KRAS^{G12C}$ Inhibition in Cancer. The New England journal of medicine, 384(25), 2382–2393. https://doi.org/10.1056/NEJMoa2105281
4. Nussinov, R., Tsai, C. J., & Jang, H. (2021). Anticancer drug resistance: An update and perspective. Drug resistance updates : reviews and commentaries in antimicrobial and anticancer chemotherapy, 59, 100796. https://doi.org/10.1016/j.drup.2021.100796
5. Jänne, P. A., Riely, G. J., Gadgeel, S. M., Heist, R. S., Ou, S. I., Pacheco, J. M., Johnson, M. L., Sabari, J. K., Leventakos, K., Yau, E., Bazhenova, L., Negrao, M. V., Pennell, N. A., Zhang, J., Anderes, K., Der-Torossian, H., Kheoh, T., Velastegui, K., Yan, X., Christensen, J. G., … Spira, A. I. (2022). Adagrasib in Non-Small-Cell Lung Cancer Harboring a KRASG12C Mutation. The New England journal of medicine, 387(2), 120–131. https://doi.org/10.1056/NEJMoa2204619
6. Hallin, J., Engstrom, L. D., Hargis, L., Calinisan, A., Aranda, R., Briere, D. M., Sudhakar, N., Bowcut, V., Baer, B. R., Ballard, J. A., Burkard, M. R., Fell, J. B., Fischer, J. P., Vigers, G. P., Xue, Y., Gatto, S., Fernandez-Banet, J., Pavlicek, A., Velastagui, K., Chao, R. C., … Christensen, J. G. (2020). The $KRAS^{G12C}$ Inhibitor MRTX849 Provides Insight toward Therapeutic Susceptibility of KRAS-Mutant Cancers in Mouse Models and Patients. Cancer discovery, 10(1), 54–71. https://doi.org/10.1158/2159-8290.CD-19-1167
7. Reck, M., Carbone, D. P., Garassino, M., &Barlesi, F. (2021). Targeting KRAS in non-small-cell lung cancer: recent progress and new approaches. Annals of oncology : official journal of the European Society for Medical Oncology, 32(9), 1101–1110. https://doi.org/10.1016/j.annonc.2021.06.001
8. Karuppasamy, M. P., Venkateswaran, S., &Subbiah, P. (2020). PDB-2-PBv3.0: An updated protein block database. Journal of bioinformatics and computational biology, 18(2), 2050009. https://doi.org/10.1142/S0219720020500092
9. Burley, S. K., Berman, H. M., Kleywegt, G. J., Markley, J. L., Nakamura, H., &Velankar, S. (2017). Protein Data Bank (PDB): The Single Global Macromolecular Structure Archive. Methods in molecular biology (Clifton, N.J.), 1607, 627–641. https://doi.org/10.1007/978-1-4939-7000-1_26
10. Seeliger, D., & de Groot, B. L. (2010). Ligand docking and binding site analysis with PyMOL and Autodock/Vina. Journal of computer-aided molecular design, 24(5), 417–422. https://doi.org/10.1007/s10822-010-9352-6
11. Dr Uma kumari, Devanshi Gupta, In silico RNA aptamer drug design and modelling,2022/4, Journal-JETIR,Volume-9, Issue-4, Pages 718-725
12. Williams, C. J., Headd, J. J., Moriarty, N. W., Prisant, M. G., Videau, L. L., Deis, L. N., Verma, V., Keedy, D. A., Hintze, B. J., Chen, V. B., Jain, S., Lewis, S. M., Arendall, W. B., 3rd, Snoeyink, J., Adams, P. D., Lovell, S. C., Richardson, J. S., & Richardson, D. C. (2018). MolProbity: More and better reference data for improved all-atom structure validation. Protein science : a publication of the Protein Society, 27(1), 293–315. https://doi.org/10.1002/pro.3330

13. Sievers, F., & Higgins, D. G. (2021). The Clustal Omega Multiple Alignment Package. Methods in molecular biology (Clifton, N.J.), 2231, 3–16. https://doi.org/10.1007/978-1-0716-1036-7_1

14. Sievers, F., & Higgins, D. G. (2018). Clustal Omega for making accurate alignments of many protein sequences. Protein science : a publication of the Protein Society, 27(1), 135–145. https://doi.org/10.1002/pro.3290

15. McGinnis S, Madden TL. BLAST: at the core of a powerful and diverse set of sequence analysis tools. Nucleic Acids Res. 2004 Jul 1;32(Web Server issue):W20-5. doi: 10.1093/nar/gkh435. PMID: 15215342; PMCID: PMC441573.

16. Buchan, D. W. A., & Jones, D. T. (2019). The PSIPRED Protein Analysis Workbench: 20 years on. Nucleic acids research, 47(W1), W402–W407. https://doi.org/10.1093/nar/gkz297

17. McGuffin, L. J., Bryson, K., & Jones, D. T. (2000). The PSIPRED protein structure prediction server. Bioinformatics (Oxford, England), 16(4), 404–405. https://doi.org/10.1093/bioinformatics/16.4.404

18. Dutil, J., Chen, Z., Monteiro, A. N., Teer, J. K., &Eschrich, S. A. (2019). An Interactive Resource to Probe Genetic Diversity and Estimated Ancestry in Cancer Cell Lines. Cancer research, 79(7), 1263–1273. https://doi.org/10.1158/0008-5472.CAN-18-2747

19. Tate JG, Bamford S, Jubb HC, Sondka Z, Beare DM, Bindal N, Boutselakis H, Cole CG, Creatore C, Dawson E, Fish P, Harsha B, Hathaway C, Jupe SC, Kok CY, Noble K, Ponting L, Ramshaw CC, Rye CE, Speedy HE, Stefancsik R, Thompson SL, Wang S, Ward S, Campbell PJ, Forbes SA. COSMIC: the Catalogue Of Somatic Mutations In Cancer. Nucleic Acids Res. 2019 Jan 8;47(D1):D941-D947. doi: 10.1093/nar/gky1015. PMID: 30371878; PMCID: PMC6323903.

20. Liu Y, Yang X, Gan J, Chen S, Xiao ZX, Cao Y. CB-Dock2: improved protein-ligand blind docking by integrating cavity detection, docking and homologous template fitting. Nucleic Acids Res. 2022 Jul 5;50(W1):W159-W164. doi: 10.1093/nar/gkac394. PMID: 35609983; PMCID: PMC9252749.